Clays and Clay Minerals, Vol. 40, No. 3, 347–354, 1992.

THE INFLUENCE OF ALUMINUM ON IRON OXIDES. PART XVI: HYDROXYL AND ALUMINUM SUBSTITUTION IN SYNTHETIC HEMATITES

HELGE STANJEK AND UDO SCHWERTMANN

Lehrstuhl für Bodenkunde der Technischen Universität München
D-8050 Freising-Weihenstephan, Germany

Abstract—Synthetic hematites with Al substitutions between 0 and 18 mol % were synthesized at different temperatures and water activities. The cell-edge lengths **a** for different synthesis conditions decreased linearly with increasing Al substitution. The regression lines, however, had different slopes and intercepts: the series with the highest synthesis temperature (1270 K) had the most negative slope. With increasing Al substitution, the hematites contained increasing amounts of non-surface water. Significant correlations were found between these chemically determined water contents and the deviations of the unit-cell parameters **a**, **c**, and **V** relative to the corresponding 1270 K regression lines. To explain the measured X-ray peak intensities, structural OH had to be included into the theoretical calculations. From intensity ratios normalized to I_{113}, it is possible to determine the structural OH separately from the Al substitution, which can be assessed by the shift of the cell-edge lengths relative to the 1270 K regression lines. The incorporation of Al and OH into the hematite structure induces strain, which was quantified by X-ray diffraction.

Key Words—Al substitution, Cell-edge lengths, Hematite, LOI, OH substitution, X-ray intensity.

INTRODUCTION

Al substitution in hematite (Forestier and Chaudron, 1925; Passerini, 1930; Brill, 1932) decreases all unit-cell parameters towards those of corundum. The cell-edge lengths of synthetic pure and Al-substituted hematites, however, exhibit substantial deviations from the Vegard line connecting the cell-edge lengths of hematite and corundum (Caillière *et al.*, 1960; von Steinwehr, 1967; Wefers, 1967; Perinet and Lafont, 1972; Schwertmann *et al.*, 1979; Barron *et al.*, 1984). To date no satisfactory explanation has been given for this observation. The synthesis temperature seems to play a role (cf. Schwertmann, 1984), because cell-edge lengths are usually lower with higher synthesis temperatures. Temperature influences the rate of the dehydroxylation, which is necessary for the growth of hematite from Fe monomers.

The purpose of this study was, therefore, to test the hypothesis that structural water might be a further factor for the aforementioned deviations. Small amounts of "water" in hematite were reported as early as 1906, when Königsberger and Reichenheim reported weight losses from single crystals of hematite from Elba.

To study the dependence of cell-edge lengths of aluminous hematites on Al substitution and water content, several series with different Al and water activities were synthesized at different temperatures. The products were characterized chemically by X-ray diffraction and infrared spectroscopy.

MATERIALS AND METHODS

Series S6

Freshly prepared solutions of 0.1 M $Fe(NO_3)_3$ and 0.1 M $Al(NO_3)_3$ were mixed (cold) in the appropriate ratios to obtain substitutions between zero and 18 mol % Al. To 200 mL of each solution, 0.1 M in Fe and Al nitrate, 80 mL ethanol were added. We then added 60 mL 1 M NaOH while stirring vigorously. The final pH was between 7.7 and 7.8. After diluting to 400 mL (0.05 M), one series was stored at 313 K for 107 days (series S6/313K), a second series at 338 K for 76 days (series S6/338K), and a third series at 363 K for 107 days (series S6/363K). All suspensions were kept in glass bottles. Experimental conditions are summarized in Table 1.

Series S8

To 200 mL solutions, 0.2 M in Fe- and Al-nitrate, 30 mL 4 M NaOH were added while stirring vigorously. The volumes were adjusted to 700 mL and centrifuged. After decanting the clear supernatant, the precipitates were resuspended in 700 mL of water and allowed to stand overnight. After further centrifugation and decantation, additional water was added to the residue and the pH and volume were adjusted to 7 ± 0.5 and 800 mL, respectively. The suspensions were stored at 313 K for 303 days in polyethylene bottles (S8/313K) and a second batch was kept at 353 K for 186 days (series S8/353K). The pH was adjusted once

a day. After one week, the pH was nearly constant and was subsequently adjusted once a week. The suspensions were shaken manually several times a week. The final precipitates were washed with distilled water, centrifuged, and freeze-dried.

1270 K series

These samples are identical to the samples described by Schwertmann *et al.* (1979) and Murad (1984), except that those had been heated to 1270 K for 47 hr. Table 1 gives a short description of all series.

Prior to analysis, all samples were treated with oxalate (Schwertmann, 1964) to remove non-converted ferrihydrite. After dissolving a 10 mg sample in 2 mL concentrated HCl, total Fe and Al were determined with sulfosalicylic acid (Koutler-Anderson, 1953) and aluminon (Hsu, 1963), respectively. Weight loss was determined by heating a 30 mg sample in a porcelain crucible first at 470 K for 24 hr and then at 1070 K for 70 hr. Loss on ignition (LOI) was taken as the difference between the weight at 470 K and at 1070 K corrected for goethite.

X-ray step scans were run from 20° to 80° 2Θ (CoKα) with a Philips vertical goniometer (PW 1050) equipped with a diffracted beam monochromator. A counting time of 10 seconds and an increment of 0.02° 2Θ were used. Elemental silicon (Merck, #12497) <20 μm with **a** = 5.43074 Å (Klug and Alexander, 1974) served as an internal standard for series S6 and S8 and as an external standard for series 1270 K. All scans were fitted with the program FIT (modified from Janik and Raupach, 1977; Schulze, 1982 by Stanjek, 1991). Cell edge lengths were calculated using the 012, 104, 110, 113, 024, 116, 214, and 300 peaks, after correcting for peak shifts due to particle size broadening (Stanjek, 1991). Instrumental broadening was determined using annealed Fe_2O_3.

Height, full width at half height, and the ratio of the Lorentz-profile to the Gaussian-profile (refined by the fitting program) were used to calculate integral intensities of the aforementioned peaks. These intensities were compared with theoretically derived intensities using the structure factor F_{hkl}:

$$F_{hkl} = 6\cdot[xf_{Fe^{3+}} + yf_{Al^{3+}} + zf_{H^+}] \cdot[\cos 2\pi lw + \cos 2\pi(lw + \tfrac{1}{2})] + 6\cdot f_{O^{2-}}[\cos 2\pi(hu + \tfrac{1}{4}) + \cos 2\pi \cdot(ku + \tfrac{1}{4}) + \cos 2\pi(hu + ku - \tfrac{1}{4})]. \quad (1)$$

The coefficients x, y, and z were calculated from the chemical formula. The atom form factors $f_{Fe^{3+}}$, $f_{Al^{3+}}$, and $f_{O^{2-}}$ were taken from Klug and Alexander (1974); f_{H^+} is zero. The parameters u = 0.3059 and w = 0.3553, which determine the positions of oxygen and iron in the structure, respectively, (Blake *et al.*, 1966), were assumed to remain constant across the solid solution. The Miller indices are h, k, and l. Isotropic temperature factors were used.

Table 1. Synthesis temperatures and time of aging of the series.

Series	Temp. K	Al (x) mol %	Storage time in days	Comments
S6	313	0–18	107	20 vol % ethanol
	338	0–18	78	20 vol % ethanol
	363	0–18	107	20 vol % ethanol
S8	313	0–18	303	no ethanol added
	353	0–8	186	no ethanol added
1270 K	1270	0–10	—	heated to 1270 K

Random substitution of Al in a crystal automatically leads to some disorder, which influences the intensities of certain reflections (cf. Guinier, 1963; Born and Paul, 1979). The resulting diffuse scattering was included in the calculations of relative intensities. (Details are given in Stanjek, 1991).

To calculate the effective particle size and strain, the measured widths at half height were corrected for instrumental broadening by applying correction-functions derived from folding procedures (Stanjek, 1991). Assuming that particle-size broadening yields Lorentzian profiles and strain broadening Gaussian profiles, both effects can be separated by the formula (from Klug and Alexander, 1974, p. 665):

$$\frac{(\delta 2\vartheta)^2}{\tan^2\vartheta_0} = \frac{K\lambda}{L}\left[\frac{\delta 2\vartheta}{\tan\vartheta_0 \sin\vartheta_0}\right] + 16e^2 \quad (2)$$

where $\delta 2\vartheta$ is the integral breadth corrected for instrumental broadening, ϑ_0 is the angle of reflection, K the Scherrer constant and λ the wavelength. L is the mean dimension of the crystallites (MCD), and e is the strain. A plot of the left side of Eq. (2) against the term in brackets on the right side would yield Kλ/L as the slope and $16e^2$ as the intercept of a linear relation from which L and e can be calculated.

For sixteen hematite samples, the infrared spectra were digitally recorded in the range from 4000 cm^{-1} to 2000 cm^{-1} using pellets prepared from 300 mg KBr and about 1 mg sample. After homogenizing for 1 minute, the powders were pressed with $8\cdot10^8$ Pa for 1 minute. Surface-bound water on the KBr and the sample itself were removed by drying the pellets at 440 K for 14 days. Preliminary experiments showed that the band intensities remained constant after this time. The digital scans, converted from percent transmission into extinction units by taking the decadic logarithm, were fitted with FIT. Three single Lorentz lines were sufficient to fit the asymmetric absorption band around 3400 cm^{-1}. The center of gravity and the area were calculated from all three lines. Additional spectra between 2000 cm^{-1} to 200 cm^{-1} were run using CsI as a solvent.

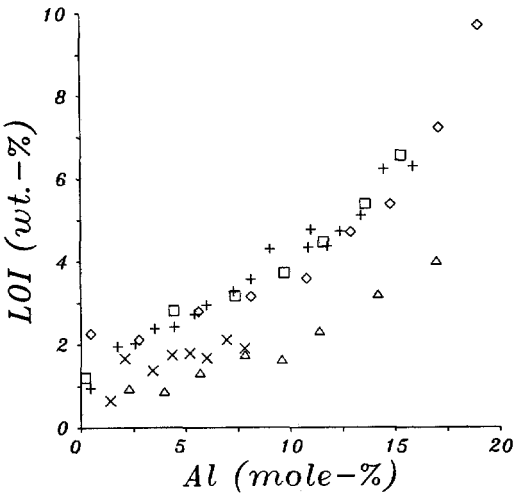

Figure 1. Loss on ignition (LOI) at 1270 K minus LOI at 470 K versus Al content in all hematites. (□ S6/313K, ◇ S6/338K, △ S6/363K, + S8/313K, × S8/353K).

Surface areas were measured with EGME (Carter *et al.*, 1965).

RESULTS

Mineralogical composition and loss on ignition

After storage all samples contained hematite and some residual ferrihydrite, which was removed by the oxalate treatment. Goethite was detected only at zero Al except in series S8/353K, which contained <2% goethite at Al substitutions up to 3 mol %.

As seen in Figure 1 LOI ranged between about 1 and 10%, and increased with increasing Al content. At a given Al content, hematites synthesized at 363 K (series S6/363K) and, to a lesser extent, those produced at 353 K (series S8/353K) contained less water than those synthesized at lower temperatures.

Cell edge lengths

Increasing Al substitution lowered the cell edge lengths **a** in all series (Figure 2) strictly linearly. The

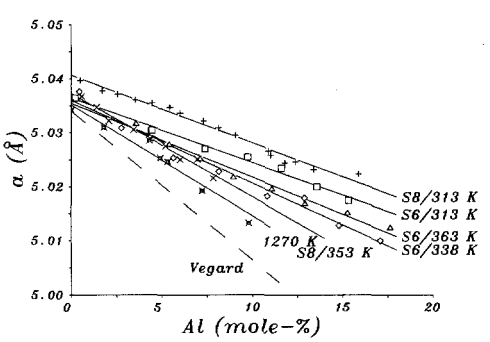

Figure 2. Cell edge, **a**, versus Al content. The broken line (V) connects **a** of pure hematite with **a** of corundum (Vegard line).

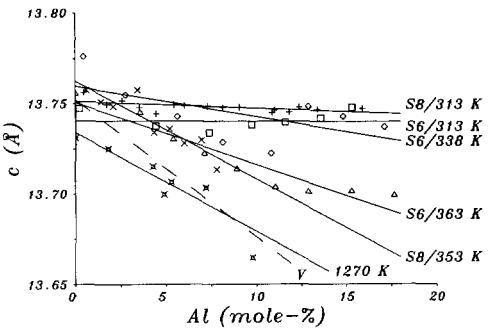

Figure 3. Cell edge, **c**, versus Al content. The broken line (V) is the Vegard line.

lines, however, varied in slope and intercept. Such behaviour has been previously described by Caillière *et al.* (1960), von Steinwehr (1967), Barron *et al.* (1984), Kosmas *et al.* (1986), and Schwertmann (1988), and has been taken as proof of Al-for-Fe substitution in the structure. In three out of six series the slopes of the regression lines deviate more from the Vegard line connecting the cell-edge of hematite and corundum with lower synthesis temperatures.

The cell edge length **c** shows an irregular decrease with Al content (Figure 3). In series S6/313K and S8/313K **c** is essentially independent of Al substitution. Again, **c** for low-temperature hematites tends to deviate more from the Vegard line than **c** for high temperature hematites.

The intercept of the regression lines in Figure 2 corresponds to the unit-cell edge **a** of pure hematite. A plot of these intercepts versus synthesis temperature—including literature data (Stanjek, 1991)—indicates two regions (Figure 4). Above 370 K no dependence exists, whereas a very good correlation was observed below

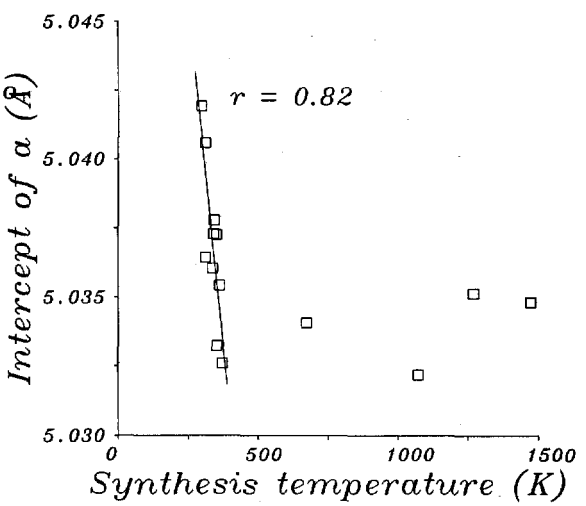

Figure 4. Intercepts of the regression lines for cell edge **a** from Figure 2 plotted versus the synthesis temperature.

https://doi.org/10.1346/CCMN.1992.0400316 Published online by Cambridge University Press

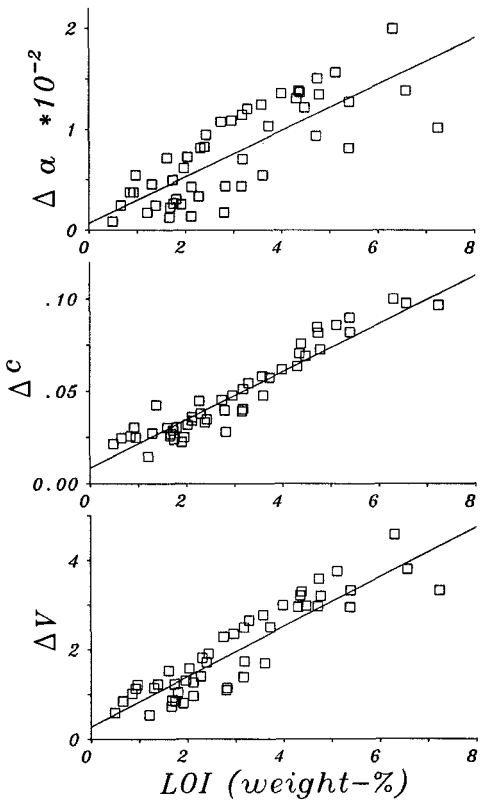

Figure 5. Differences between the measured cell parameters of series S6 and S8 and the theoretical water-free values taken from the 1270 K regression line plotted versus the LOI.

370 K (Intercept **a** = 5.0703 − $9.858 \cdot 10^{-5} \cdot T_{synth.}$; r = 0.82; n = 10).

To explain the variation of the cell-edge lengths at a given Al substitution, structural water was included as a further variable. The regression lines of **a**, **c**, and **V** of the 1270 K samples served as a reference for water-free hematites. For all other hematites, the differences (Δ**a**, Δ**c**, Δ**V**) between the cell parameters at any given synthesis temperature and those of the reference samples were calculated and plotted against LOI (Figure 5).

Although highly significant correlations (Table 2) were found for all these Δ values for all series (Figure 5), the correlation for Δ**c** was higher than for Δ**a**. The Δ values of individual series were also significantly correlated with the corrected LOI except in series S8/535K, where the variation of the weight losses (0 − 2.1 wt. %) was probably too small.

Infrared spectra

Prior to drying, the samples showed an intense and asymmetric absorption band at 3420 cm^{-1} and a band at 1680 cm^{-1} due to adsorbed molecular water. After drying at 440 K, all 16 hematites still showed a broad and skewed band with maximum absorption around 3400 cm^{-1}, whereas only a weak feature remained around 1650 cm^{-1}. Rochester and Topham (1979) assigned the 3400 cm^{-1} band to stretching and bending of surface OH. The areas (Figure 6) of this band, however, correlate significantly with LOI after drying (r = 0.91, n = 16, p = 0.001). The positive intercept of 0.070 ± 0.036 of this correlation is statistically not different from zero. The regressions of LOI versus surface area (r = 0.75, n = 16, p = 0.01) and the IR band areas versus surface area (r = 0.67, n = 16, p = 0.05) are also significant. The lower significances of the two latter regression lines, however, indicate that the major contribution to the stretching band intensity originates from structural rather than from surface OH.

A band in the range between 900 to 1000 cm^{-1}, which was assigned to OH vibrations in "hydrohematite" (Wolska, 1981; Wolska and Szajda, 1985) was not observed in the CsI spectra. A further band at 630 cm^{-1}, observed by Wolska (1981), is more likely due to the O^{2-} displacement mode E_g (Farmer, 1974), which shifts with increasing Al substitution from 615 to 650 cm^{-1} (Barron *et al.*, 1984).

Table 2. Coefficients for the regressions of Δ**a**, Δ**c**, and Δ**V** versus Loss on ignition (LOI) (56 samples).

Δ**a** = 0.0006793 + 0.002298 · LOI	r = .814
Δ**c** = 0.008411 + 0.01305·LOI	r = .933
Δ**V** = 0.2690 + 0.5593·LOI	r = .907

All correlation coefficients are significant at the <0.001 level.

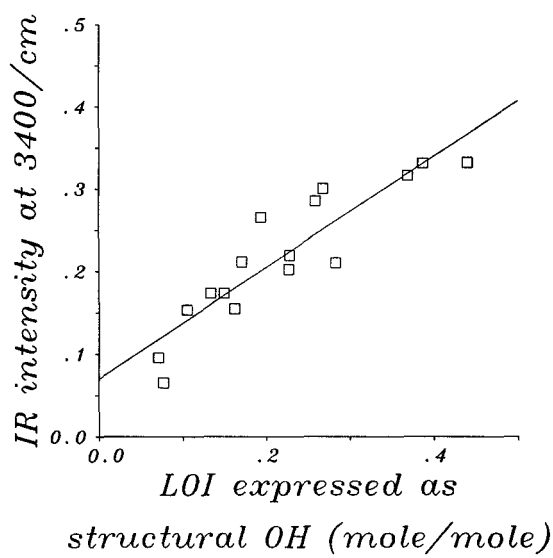

Figure 6. Integrated intensities of the infrared absorption bands at 3400 cm^{-1} plotted versus LOI expressed as structural OH (i.e., in $(Fe_{1-x}Al_x)_{2-z/3}(OH)_zO_{3-z}$).

https://doi.org/10.1346/CCMN.1992.0400316 Published online by Cambridge University Press

Table 3. Regression parameters of the changes of the intensity ratios with structural contents of Al and OH: $I_{hkl}/I_{113} = a \cdot x + b \cdot z + c$, where x and z refer to the formula $(Fe_{1-x}Al_x)_{2-z/3}(OH)_zO_{3-z}$.

Intensity ratio hkl/113	Intensity ratios						
	Calculated			Measured			
	a	b	c	a	b	c	r[1]
012	−128.4	−91.1	139.2	−132.9	−126.0	124.2	0.942
104	−531.8	−404.5	443.7	280.9	−385.9	368.1	0.780
110	−462.5	−367.1	310.7	−382.6	−144.9	−208.1	0.909
024	−170.9	−131.6	170.7	−169.6	−140.1	138.5	0.958
116	−173.1	−131.1	207.4	−335.2	−40.6	160.7	0.422
214	−142.5	−114.0	139.7	−146.3	−102.8	108.1	0.857
300	−108.2	−83.2	137.1	−220.4	−33.4	114.2	0.818

[1] Regression coefficients for the intensity ratios $I_{hkl\ meas.}/I_{hkl\ calc.}$.

XRD intensities

The structure factor F_{hkl} determines the relative intensities of X-ray reflections and includes, apart from the structural terms *sensu stricto,* the chemistry of the crystal. Wolska (1981) first demonstrated that substitution of Fe^{3+} by Al^{3+} in hematites can be detected by changes in peak intensities relative to that of 113, whose intensity is independent of the cations. In our study the amount of structural OH was included in the intensity calculations [cf. Eq. (1)]. The influence of diffuse scattering was also considered, because the "mean" atom form factor in the above equation does not account for the influence of random cation distribution. This produces diffuse scattering, whose intensity I_2 is a function of the differences between the atom form factors of the substituting cations Al and H, and that of Fe (cf. Guinier, 1963; Born and Paul, 1979). We calculate I_2 as:

$$I_2 = \overline{|F_n|^2} - \overline{|F_{hkl}|^2} \qquad (3)$$

with

$$\overline{|F_n|^2} = x_{Fe} \cdot f^2_{Fe} + x_{Al} \cdot f^2_{Al} + x_H \cdot f^2_H. \qquad (4)$$

The calculated intensities were normalized to the 113.

Significant correlations were found between the measured and the calculated intensities. The slopes, however, deviate from 1. For the 116 reflection no relationship was found. The inclusion of the diffuse scattering generally improved the relationships.

Al and OH always decrease the theoretical intensities relative to 113. Significant multiple correlations between the structural Al and H contents and the measured intensity ratios I_{hkl}/I_{113} were found, except for the ratio I_{116}/I_{113} (Table 3). The coefficients obtained from the calculated intensities differ statistically in some cases from the theoretical values (cf. Table 3), especially for 104/113 and 116/113.

Since a single intensity ratio depends on both Al and H, Al and H can be calculated by combining two regression equations taken from Table 3. Mean contents of Al and of H calculated using all possible combinations of these intensity ratios correlate significantly with the chemically determined contents (Figure 7) (Al: r = 0.761; H: r = 0.934, n = 41). The slopes do not deviate from 1. The three extraneous values in Figure 7 (right side) were excluded from the regression analysis. These samples contain goethite and, according to their measured intensities, should not contain OH. The high measured contents of OH, therefore, are probably due to systematic errors in the quantification of the goethite content.

Strain

The substitution of Al^{3+} for Fe^{3+} should induce strain, because the Al–O bonds are shorter than the Fe–O bonds. The replacement of 3 O^{2-} by 3 OH^- in a vacant site also induces strain, because all three hydrogens are not necessarily located within one octahedral site. A plot of strain, calculated from 012 and 024, against Al content (Figure 8) shows a nonlinear increase very similar to LOI (Figure 1). Assuming a linear influence of Al content upon strain, the nonlinear behaviour may be explained by an increasing incorporation of OH into the hematite structure.

DISCUSSION

The significant correlations between the cell-parameter deviations from the ideal cell size, the loss of ignition, and the infrared band intensities indicate that, apart from Al, "water" is also located in the crystal structure of hematite in the form of hydroxyl groups (Gregg and Hill, 1953; Okamoto *et al.,* 1967; Wolska, 1977, 1981; Wolska and Szajda, 1985). This is also supported by the intensity changes of the XRD peaks, which cannot be explained without assuming the presence of additional protons in the structure. OH-for-O substitution (expressed as H_2O) exceeds Al substitution by far. In some highly (>15 mol %) Al substituted hematites the ratio (Fe+Al)/OH approaches unity, i.e., a magnitude similar to that in goethite.

Using all samples from this study in multiple correlations, more than 80% of the variations of **a**, **c**, and

https://doi.org/10.1346/CCMN.1992.0400316 Published online by Cambridge University Press

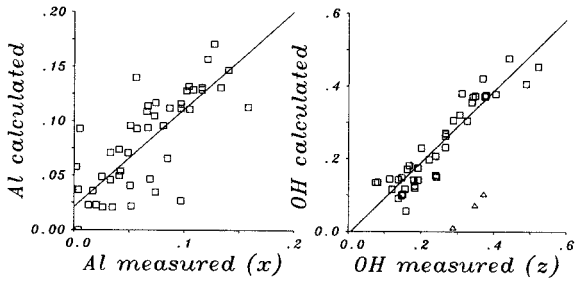

Figure 7. Measured contents of Al (left) and H (right) versus calculated (from XRD intensities) content according to the formula $(Fe_{1-x}Al_x)_{2-z/3}(OH)_zO_{3-z}$. The three values marked with △ contain goethite and were not included in the regression.

V can be explained by Al and OH substitution (Table 4). Within experimental error, the coefficients for the Al substitution are identical to those of the 1270 K regression line. This is due to the fact that the deviations of the cell parameters from this line are correlated with the LOI.

From the regressions in Figure 5 it can be concluded that the deviation of **c** from the ideal structure is much better correlated with LOI than **a** is. The poor correlation of **c** with Al content observed by various authors can thus be explained by the fact that **c** is more affected by structural OH than **a**. In corundum the OH dipole probably lies in a plane perpendicular to the c-axis, where an oxygen common to two face-sharing octahedra may serve as a donator for OH (Beran, 1991). The model might be different for hematite, however, because of the much higher cation deficiencies.

As indicated by the signs of the regression coefficients in Table 4, OH—in contrast to Al—enlarges the unit cell size towards that of ferrihydrite. In comparison to the mechanism of cation substitution, which is (in this case) restricted to identical sites within the structure, the mechanism of anion substitution seems to be different. On an average, the structure contains 2.2 OH per Al. This presence of OH for Al can be explained by the standard free energy changes of the dehydration which are as follows, for the corresponding monomers (Gibbs free energy data from Helgeson *et al.*, 1978, and from Lindsay, 1979):

$$Fe(OH)^0_3 \rightleftharpoons \tfrac{1}{2}\,Fe_2O^s_3 + \tfrac{3}{2}\,H_2O^l \cdot(\Delta G_r = -84\ kJ/mol) \qquad (5)$$

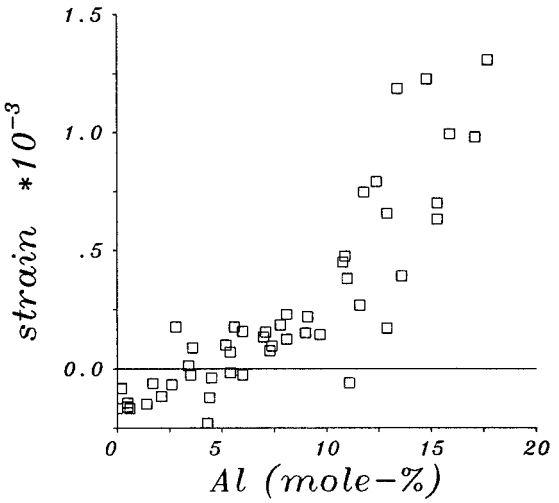

Figure 8. Strain (calculated with Eq. (2)) versus Al substitution. Negative values are due to small systematic errors in the correction for instrumental broadening.

and

$$Al(OH)^0_3 \rightleftharpoons \tfrac{1}{2}\,Al_2O^s_3 + \tfrac{3}{2}\,H_2O^l \cdot(\Delta G_r = +13\ kJ/mol). \qquad (6)$$

The growth of hematite is thus thermodynamically favored over that of corundum. However, even unsubstituted hematites contain OH, the amount of which depends on the synthesis temperature and thus on the rate of formation.

With increasing Al substitution, LOI increases overproportionately (cf. Figure 1). This behaviour might be explained by the probability of finding two or more neighbouring Al cations in the structure, which increases overproportionately with increasing Al substitution (Stanjek, 1991). The dehydroxylation of an $Al(OH)^0_3$ monomer might therefore be less complete, as more surface-attached Al is surrounded by other Al cations, due to the polarizing effects of its neighbours. Extrapolated to a pure Al hydroxide, no Al_2O_3 should form under ambient conditions, which agrees with the fact that corundum has been found in soils only after burning events (Anand and Gilkes, 1987; Stanjek, 1987).

Several factors account for the residual variances of the XRD peak intensities: (1) preferred orientation due to the platy morphology of the crystals enhances re-

Table 4. Multiple regression equations for the cell parameters as a function of Al and LOI (48 samples).

a = 5.0359(29) − 0.00183(15)·Al[1] + 0.00175(45)·LOI[2]	r = 0.923
c = 13.740(7) − 0.00512(37)·Al + 0.0130(11)·LOI	r = 0.898
V = 301.78(42) − 0.330(22)·Al + 0.493(65)·LOI	r = 0.932

[1] In mol %.
[2] In wt. %.

https://doi.org/10.1346/CCMN.1992.0400316 Published online by Cambridge University Press

flections like 104 or 116 and depresses reflections like 110 or 300; (2) the parameters u = 0.3059 and w = 0.3553 (Blake *et al.*, 1966), which determine the positions of oxygen and iron in the structure, respectively, change with increasing substitution towards the parameters of corundum (u = 0.3064, w = 0.3521; Hill and Madsen, 1986). This leads to systematic intensity changes, which were neglected here. Further influences may stem from relaxations of surface oxygen and iron atoms (Mackrodt *et al.*, 1987). Deviations from the theoretical positions not only affect the relative intensities but may also induce strain broadening.

We should discuss the reason for the unusually long heating time—several days (Wolska, 1977; Wolska and Szajda, 1985)—which was necessary to completely expel OH from the structure. Above 470 K, OH groups on the surface are driven off as water molecules. The diffusion of protons from within the structure to the surface leads to an enrichment of Fe^{3+} near the surface, where oxygens and hydrogens are lost as water. The resulting charge imbalance then creates the driving force for the diffusion of Fe^{3+} towards the interior of the crystal to compensate for the positive charges lost. According to Tamman's theory (cf. Gregg, 1953), however, volume diffusion only starts above the "Tamman temperature", which should be at approximately half the melting point of 1838 K. This leads to a very high activation energy of 390–580 kJ/mol for cation diffusion in hematite (Catlow *et al.*, 1988).

CONCLUSIONS

Synthetic pure and Al-substituted hematites contain appreciable amounts of OH, which counteracts the effect of Al to reduce the cell size. Increasing incorporation of protons decreases the relative XRD peak intensities. It is therefore possible to determine the structural OH and Al from X-ray peak intensities.

In spite of the presence of structural OH, we hesitate to revive the term "hydrohematite" (Breithaupt, 1847), because there is no principal structural difference from "hematite". A more precise and unambiguous characterization for such hematites should be the general formula $(Fe_{1-x}Al_x)_{2-z/3}(OH)_zO_{3-z}$.

ACKNOWLEDGMENTS

The authors thank E. Murad for many valuable discussions and for improving the manuscript. This work was financed by the Deutsche Forschungsgemeinschaft.

REFERENCES

Anand, R. R. and Gilkes, R. J. (1987) The association of maghemite and corundum in Darling Range laterites, Western Australia: *Aust. J. Soil Res.* **25,** 303–311.

Barron, V., Rendon, J. L., Torrent, J., and Serna, C. J. (1984) Relation of infrared, crystallochemical, and morphological properties of Al-substituted hematites: *Clays & Clay Minerals* **32,** 475–479.

Beran, A. (1991) Trace hydrogen in Verneuil-grown corundum and its colour varieties—An IR spectroscopic study: *Eur. J. Mineral.* **3,** 971–975.

Blake, R. L., Hessevick, R. E., Zoltai, T., and Finger, L. W. (1966) Refinement of the hematite structure: *Amer. Mineral.* **51,** 123–129.

Born, E. and Paul, G. (1979) *Röntgenbeugung am Realkristall:* Thieme Verlag, München, 155 pp.

Breithaupt, A. (1847) *Handbuch der Mineralogie, Band III:* Arnoldi, Dresden.

Brill, R. (1932) Röntgenographische Untersuchungen an Eisenkatalysatoren für die Ammoniak-Synthese: *Z. Elektrochemie* **38,** 669–673.

Cailliére, S., Gatineau, L., and Hénin, S. (1960) Préparation a basse temperature d'hématite alumineuse: *Comptes Rendus Acad. Sci.* **250,** 3677–3679.

Carter, D. L., Heilman, M. D., and Gonzales, C. L. (1965) The ethylene glycol monoethyl ether (EGME) technique for determining soil-surface area: *Soil Sci.* **100,** 409–413.

Catlow, C. R. A., Cornish, J., Hennesy, J., and Mackrodt, W. C. (1988) Atomistic simulation of defect structures and ion transport in α-Fe_2O_3 and α-Cr_2O_3: *J. Amer. Ceram. Soc.* **71,** 42–49.

Farmer, V. C. (1974) The anhydrous oxide minerals: in *The Infrared Spectra of Minerals,* V. C. Farmer, ed., Mineralogical Society, London, 539 pp.

Forestier, H. and Chaudron, G. (1925) Points de transformation des solutions solides d'alumine ou de sesquioxyde de chrome dans les sesquioxyde de fer: *Comptes rendus Acad. Sci. Paris* **180,** 1264–1266.

Gregg, S. J. (1953) The production of active solids by thermal decomposition. Part I. Introduction: *J. Chem. Soc.* **IV,** 3940–3944.

Gregg, S. J. and Hill, K. J. (1953) The production of active solids by thermal decomposition. Part II. Ferric oxide: *J. Chem. Soc.* **IV,** 3945–3951.

Guinier, A. (1963) *X-ray Diffraction in Crystals, Imperfect Crystals and Amorphous Bodies:* Freeman and Company, San Francisco, 378 pp.

Helgeson, H. C., Delany, J. M., Nesbitt, H. W., and Bird, D. K. (1978) Summary and critique of the thermodynamic properties of rock-forming minerals: *Amer. J. Sci.* **278A,** 1–229.

Hill, R. J. and Madsen, I. C. (1986) The effect of profile step width on the determination of crystal structure parameters and estimated standard deviations by X-ray Rietveld analysis: *J. Appl. Crystall.* **19,** 10–18.

Hsu, P. H. (1963) Effect of initial pH, phosphate, and silicate on the determination of aluminum with aluminon: *Soil Sci.* **96,** 230–237.

Janik, L. M. and Raupach, M. (1977) An iterative, least-squares program to separate infrared absorption spectra into their component bands: *CSIRO Div. of Soils Tech. Paper* **35,** 1–37.

Klug, H. P. and Alexander, L. E. (1974) *X-Ray Diffraction Procedures for Polycrystalline and Amorphous Materials:* J. Wiley and Sons, New York, 966 pp.

Königsberger, J. and Reichenheim, O. (1906) Ueber die Elektrizitätsleitung einiger natürlich kristallisierter Oxyde and Sulfide und des Graphits: *N. Jb. Min. Geol. Pal. 1906*

Kosmas, C. S., Franzmeier, D. P., and Schulze, D. G. (1986) Relationship among derivative spectroscopy, color, crystallite dimensions and Al substitution of synthetic goethites and hematites: *Clays & Clay Minerals* **34,** 625–634.

Koutler-Anderson, E. (1953) The sulfosalicylic method for iron determination and its use in certain soil analysis: *Ann. Roy. Agric. Sweden* **20,** 297–308.

Lindsay, W. L. (1979) *Chemical Equilibria in Soils:* J. Wiley & Sons, New York, 449 pp.

Mackrodt, W. C., Davey, R. J., Black, S. N., and Docherty, R. (1987) The morphology of α-Al_2O_3 and α-Fe_2O_3: The importance of surface relaxation: *J. Cryst. Growth* **80,** 441–446.

Murad, E. (1984) High-precision determination of magnetic hyperfine fields by Mössbauer spectroscopy using an internal standard: *J. Phys. E. Sci. Instrum.* **17,** 736–737.

Okamoto, G., Furuichi, R., and Sato, N. (1967) Chemical reactivity and electrical conductivity of hydrous ferric oxide: *Electrochim. Acta* **12,** 1287–1299.

Passerini, L. (1930) Soluzione solide, isomorfismo e simmorfismo tra gli ossidi dei metalli trivalenti. I sistema: Al_2O_3-Cr_2O_3; Al_2O_3-Fe_2O_3: Cr_2O_3-Fe_2O_3: *Gazz. Chim. Ital.* **60,** 544–558.

Perinet, G. and Lafont, R. (1972) Sur les parametres cristallographiques des hématites alumineuses: *Comptes Rendus Acad. Sci. Paris* **275 C,** 1021–1025.

Rochester, C. H. and Topham, S. A. (1979) Infrared study of surficial hydroxyl groups on haematite: *J. Chem. Soc., Faraday Trans.* **I 75,** 1073–1088.

Schulze, D. G. (1982) The identification of iron oxides by differential X-ray diffraction and the influence of aluminum substitution on the structure of goethite: Ph.D. thesis, Technische Universität München, University Microfilms International, Ann Arbor, Michigan, 167 pp.

Schwertmann, U. (1964) Differenzierung der Eisenoxide des Bodens durch photochemische Extraktion mit saurer Ammoniumoxalat-Lösung: *Z. Pflanzenernähr. Bodenkde.* **105,** 194–202.

Schwertmann, U. (1984) Aluminiumsubstitution in pedogenen Eisenoxiden—eine Übersicht: *Z. Pflanzenernähr. Bodenkde.* **147,** 385–399.

Schwertmann, U. (1988) Goethite and hematite formation in the presence of clay minerals and gibbsite at 25°C: *Soil Sci. Soc. Amer. J.* **52,** 288–291.

Schwertmann, U., Fitzpatrick, R. W., Taylor, R. M., and Lewis, D. G. (1979) The influence of aluminium on iron oxides. Part II. Preparation and properties of Al-substituted hematites: *Clays & Clay Minerals* **27,** 105–112.

Stanjek, H. (1987) The formation of maghemite and hematite from lepidocrocite and goethite in a Cambisol from Corsica: *Z. Pflanzenernähr. Bodenkde.* **150,** 314–318.

Stanjek, H. (1991) Aluminium- und Hydroxylsubstitution in synthetischen und natürlichen Hämatiten: Ph.D. thesis, Technische Universität München, Maria Leidorf, Buch am Erlbach, 200 pp.

von Steinwehr, H. E. (1967) Gitterkonstanten im System α- $(Al,Fe,Cr)_2O_3$ und ihr Abweichen von der Vegardregel: *Z. Kristallographie* **125,** 377–403.

Wefers, K. (1967) Phasenbeziehungen im System Al_2O_3–Fe_2O_3–H_2O: *Erzmetall* **20,** 13–19.

Wolska, E. (1977) Die Bedeutung von Aluminiumspuren im Alterungsvorgang von amorphem Eisen(III)-hydroxid für die Eliminierung der Goethitphase: *Monatshefte Chemie* **108,** 819–828.

Wolska, E. (1981) The structure of hydrohematite: *Z. Kristallographie* **154,** 69–75.

Wolska, E. and Szajda, W. (1985) Structural and spectroscopic characteristics of synthetic hydrohematite: *J. Mater. Sci.* **20,** 4407–4412.

(Received 17 February 1992; accepted 12 May 1992; Ms. 2187)